Surg Radiol Anat (2017) 39:77–83
DOI 10.1007/s00276-016-1698-6

ORIGINAL ARTICLE

Neuromuscular structure of the tibialis anterior muscle for functional electrical stimulation

Kyu-Ho Yi[1] · Liyao Cong[2] · Jung-Hee Bae[2] · Eun-Sook Park[3] · Dong-wook Rha[3] · Hee-Jin Kim[2]

Received: 31 January 2016 / Accepted: 12 May 2016 / Published online: 20 May 2016

Abstract
Purpose This study describes the nerve entry points and intramuscular nerve branching of the tibialis anterior, providing essential information for therapeutic functional electrical stimulation and botulinum toxin injection.
Methods One hundred and ten legs from Korean and Thai cadavers were dissected. Ten specimens were harvested and subjected to modified Sihler's staining.
Results The average total length from the lateral malleolus to the fibular head was 32.0 cm (SD 1.9). The nerve entry points were densely distributed between 86.5 and 90.6 % of the reference length, where the first and second nerve entry points were observable. A densely arborizing area of the intramuscular nerve branches was observed at 70–80 % of the reference length.
Conclusions Based on the results of this study, clinicians can increase the effectiveness of therapeutic functional electrical stimulation and identify the ideal sites for botulinum toxin injection to the tibialis anterior muscle.

✉ Dong-wook Rha
medicus@yuhs.ac

✉ Hee-Jin Kim
hjk776@yuhs.ac

[1] School of Medicine, The Catholic University of Korea, Seoul, South Korea

[2] Division in Anatomy and Developmental Biology, Department of Oral Biology, Human Identification Research Center, BK21 PLUS Project, Yonsei University College of Dentistry, 50-1 Yonsei-ro, Seodaemun-gu, Seoul 03722, South Korea

[3] Department and Research Institute of Rehabilitation Medicine, Severance Rehabilitation Hospital, Yonsei University College of Medicine, 50-1 Yonsei-ro, Seodaemun-gu, Seoul 03722, South Korea

Keywords Tibialis anterior · Sihler's staining · Functional electrical stimulation · Spasticity · Botulinum toxin

Introduction

Up to 30 % of patients with cerebral vascular accidents experience foot drop as a result of impaired control of the ankle musculature, making it a major disability in rehabilitation [5, 30]. Impaired foot clearance caused by foot drop contributes to high risk of stumbling and falling, instability of gait, limited functional mobility, and unwanted compensatory gait patterns.

Functional electrical stimulation (FES) was first introduced in 1961 to correct foot drop and has now become one of the standard approaches of treating patients with foot drop [28]. FES is a useful therapeutic option, as it improves motor reaction time, isometric torque, and alternating contractions of agonist and antagonist muscles in patients with stroke [6, 10].

Various electrode positions can be used to elicit the required muscle contraction to promote ankle dorsiflexion and improve swing-phase foot clearance [3, 11, 21, 31, 34, 41, 42, 46]. One commonly used method is to place one electrode over the common fibular nerve, just below the head of the fibula, and the second electrode over the dorsiflexors [44]. The common fibular nerve has two branches: the superficial fibular branch and the deep fibular branch [1]. The tibialis anterior muscle, exerting as a strong ankle dorsiflexor and invertor, is innervated by the deep fibular nerve branch. The fibularis longus and brevis, exerting as ankle plantarflexors and evertors, are innervated by the superficial fibular nerve branch. If the stimulation of the common fibular nerve produces too much eversion of

ankle, the electrode can be relocated to stimulate the motor points of the tibialis anterior muscles [40].

It is crucial to note the neuromuscular structures of the tibialis anterior when applying electrical currents for treatments. For maximum contraction of the tibialis anterior muscle and minimum contraction of unintended fibularis muscles, the optimal intensity of electrical stimulation should be applied precisely to the nerve branch innervating the muscle. Therefore, the electrode must be ideally positioned and sized when stimulating the tibialis anterior muscle to obtain the desired responses with minimal stimulation intensity.

Spasticity of the tibialis anterior muscle has been considered as a contributor of varus deformity of the ankle in patients with central nervous system damage [32]. Clinically, ankle plantarflexors and invertors, such as the tibialis posterior, flexor digitorum longus, and flexor hallucis longus muscles, are more often targeted to correct varus deformity of the foot [37, 38]. If this fails to correct the varus deformity fully, the tibialis anterior can be injected [35]. Split anterior tibialis tendon transfer (SPLATT) is a popular surgical procedure for the treatment of the spastic equinovarus foot deformity as well [13, 29].

The aim of this study was to clarify the anatomic courses and distribution of the extramuscular and intramuscular nerves innervating the tibialis anterior muscle via topographic examination followed by detailed dissection and Sihler's staining.

Methods

Anatomical examinations were performed on 110 specimens (55 right side and 55 left side) of embalmed adult Korean cadavers (42 male, 24 female; age in years: range 43–96, mean 73.5, SD 13.8) and Thai cadavers (36 male, 8 female; age in years: range 41–93, mean 74.8, SD 14.0). The skin of the distal leg was delicately removed, and the subcutaneous tissue was removed to disclose the tibialis anterior. The extensor digitorum longus and extensor hallucis longus were carefully distracted to reveal the deep fibular nerve. After a detailed dissection, the most prominent point of the lateral malleolus and the fibular head were aligned vertically and defined as the *Y*-axis. The horizontal line crossing the lateral malleolus was defined as the *X*-axis (Fig. 1).

Nerve entry points (NEPs) were defined as locations where a nerve penetrated into the muscle belly. Musculotendinous junctions, where muscles became tendons, were pinpointed and then measured at two points: the proximal musculotendinous junction (PMTJ), where the most proximal point of the tendinous portion appeared, and the distal musculotendinous junction (DMTJ), where the most distal part of the transition point appeared. The length (from the most proximal point of the tibialis anterior origin to the LMTJ) and the width (at a point located at 70 % of the total distance from the lateral malleolus to the fibular head) of the muscle belly were also measured.

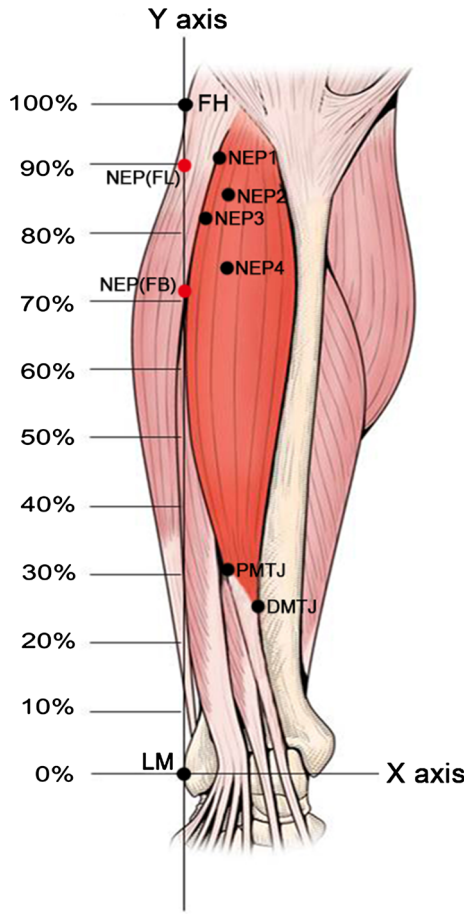

Fig. 1 Nerve entry points from the deep fibular nerve. The anatomical landmarks of the tibialis anterior were measured with the lateral malleolus as the zero point. The *X-axis* was drawn horizontally across the lateral malleolus. The *Y-axis* was drawn from the lateral malleolus to the fibular head. *LM* lateral malleolus, *FH* fibular head, *NEP1* first nerve entry point, *NEP2* second nerve entry point, *NEP3* third nerve entry point, *NEP(FL)* nerve entry point of fibularis longus, *NEP(FB)* nerve entry point of fibularis brevis, *PMTJ* proximal musculotendinous junction, *DMTJ* distal musculotendinous junction. NEP(FL) and NEP(FB) is referred from the research of Lee et al. [25]

The following locations were measured along the X-axis and Y-axis to identify their anatomical position using a protractor and digital caliper capable of measuring to the nearest 0.01 cm: the fibular head, first nerve entry point (NEP1), second nerve entry point (NEP2), third nerve entry point (NEP3), fourth nerve entry point (NEP4), proximal musculotendinous junction (PMTJ), and distal musculotendinous junction (DMTJ). All measurements along the Y-axis were converted to a percentage of the total distance from the lateral malleolus to the fibular head (the reference distance).

Staining

Sihler's method was applied to ten tibialis anterior muscles harvested from the Korean cadavers (5 male, 5 female; age in years: range 63–73, mean 67.5, SD 7.8) to observe the intramuscular nerve distribution patterns. The method included the following steps for fixation, decalcification, staining, destaining, neutralization, and clearing [47–52].

For Sihler's neutral staining, the harvested muscles were fixed by immersion in 10 % unneutralized formalin for 1 month. After fixation, the specimens were washed in running water and then placed in 3 % aqueous potassium hydroxide solution with 0.2 ml 3 % hydrogen peroxide for 4 weeks. The depigmented muscles were then transferred into Sihler's solution I, consisting of glacial acetic acid, glycerin, and 1 % aqueous chloral hydrate. Then, the muscles were dyed for 3–4 weeks in Sihler's solution II, which comprised Ehrlich's hematoxylin, glycerin, and 1 % aqueous chloral hydrate. After the staining processes, the specimens were transferred into Sihler's solution I and stirred lightly. The solution was changed when it became purple. This process ended when the stained nerve branches were clearly visible. The destained muscles were neutralized by 0.05 % lithium carbonate solution for 1 h and then washed in running water for 1 h. Subsequently, the specimens were soaked in a series of increasing concentrations (40, 60, 80, and 100 %) of glycerin.

After the staining processes, the results were compared by dividing the reference length into 10 equal sections and observing and measuring the locations of the densely sited neuromuscular junctions and the distal end point of the intramuscular nerve.

Statistical analysis

Comparisons among the cadavers based on sex were performed using independent t tests. P values <0.05 were considered statistically significant. All measurements were analyzed using SPSS version 15.0.

Results

The tibialis anterior had branches with one to four NEPs (mean 1.9; SD 0.7). One NEP was found in 30.9 % of the specimens, two NEPs were found in 53.6 % of the specimens, three NEPs were found in 13.6 % of the specimens, and four NEPs were found in only 1.8 % of the specimens. The average length of the muscle belly was 22.7 cm (SD 2.1 cm), and the average width was 2.7 cm (SD 0.4 cm), with no significant differences between the sexes.

The anatomical locations of the NEPs, PMTJ, and DMTJ are summarized in Table 1 and depicted in Figs. 1 and 2. In terms of percentages of the reference distance, the average locations of NEP1, NEP2, NEP3, and NEP4 were 90.6 % (SD 3.4 %), 86.5 % (SD 3.4 %), 82.4 % (SD 3.1 %), and 74.8 %, respectively (Fig. 1). On the X-axis of the most prominent point of lateral malleolus, NEP1, NEP2, NEP3, and NEP4 were located at 1.3 cm (SD 0.1 cm), 1.4 cm (SD 0.1 cm), 1.3 cm (SD 0.9 cm), and 1.6 cm from the reference point of lateral malleolus, respectively. The average position of the PMTJ as a percentage of the reference length was 30.0 % (SD 4.9 %), and that of the LMTJ was 25.7 % (SD 4.4 %). The Sihler's depigmenting process revealed, however, that the actual mean location of the PMTJ was at 78.2 % of the reference length.

Table 1 Anatomical points for tibialis anterior muscle

Length from LM	N	Mean (X-axis, Y-axis)	SD (X-axis, Y-axis)	Percentage distance	
				Mean (%)	SD (%)
FH	110	0, 32.0	0, 1.9	100	
NEP1	110	1.3, 29.0	0.1, 1.2	90.6	3.4
NEP2	93	1.4, 27.7	0.1, 1.2	86.5	3.4
NEP3	17	1.3, 26.4	0.9, 1.0	82.4	3.1
NEP4[a]	2	1.6, 24.0		74.8	
PMTJ	110	2.2, 10.0	0.1, 2.7	30.9	4.9
DMTJ	110	3.3, 8.2	0.1, 2.5	25.7	4.4

The nerve entry points, proximal musculotendinous junction, and distal musculotendinous junction were measured (in cm) according to the X-axis (horizontal line crossing the lateral malleolus) and Y-axis (vertical line from the lateral malleolus to the fibular head)

The percentage is based on the total distance from the fibular head to the lateral malleolus

LM lateral malleolus, *FH* fibular head, *NEPs* nerve entry points, *PMTJ* proximal musculotendinous junction, *DMTJ* distal musculotendinous junction

[a] SD was not measured because there were only two specimens

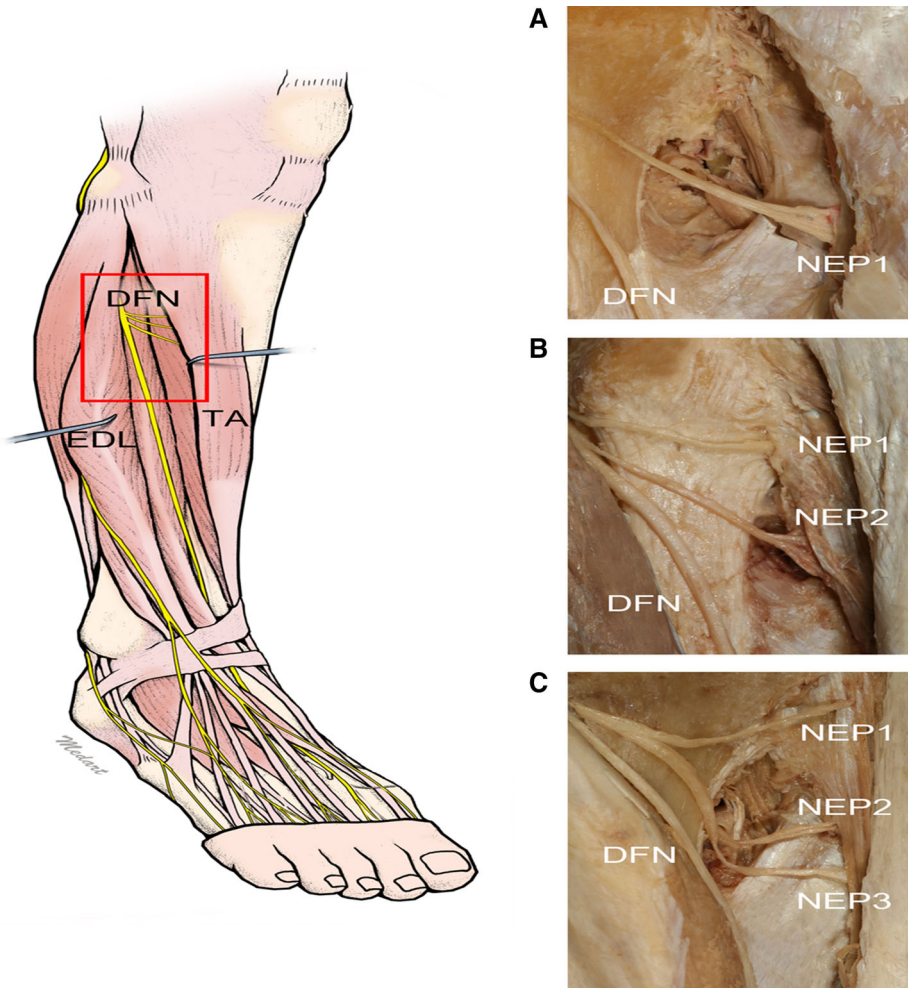

Fig. 2 Anatomical structures based on percentages regarding the lateral malleolus and fibular head. The deep fibular nerve runs down between the tibialis anterior and the extensor digitorum longus. The descending deep fibular nerve branches out to the first nerve entry point, second nerve entry point, and third nerve entry point of the tibialis anterior. Examples of muscles with one nerve entry point (**a**), two nerve entry points (**b**), and three nerve entry points (**c**) are shown. *LM* lateral malleolus, *FH* fibular head, *TA* tibialis anterior, *EDL* extensor digitorum longus, *DFN* deep fibular nerve, *NEP1* first nerve entry point, *NEP2* second nerve entry point, *NEP3* third nerve entry point

The intramuscular branching appeared to have a minimum of two and a maximum of five branches located at 80–90 % of the reference distance. Arborizing patterns appeared as those fine branches ran down distally. The intramuscular neural arborized areas were located at 70–80 % of the reference length. The most distally located intramuscular nerve ending was observed at around 25–30 % of the reference length (Fig. 3).

Comparisons between the male and female cadavers were made proportional to the height. There were no significant differences between the sexes in the location of the fibular head, NEP1, NEP2, NEP3, NEP4, PMTJ, or DMTJ.

Discussion

The tibialis anterior is located in the anterior portion of the distal leg that originates from the proximal two-thirds of the tibial body and inserts into the medial cuneiform. It is a muscle commonly targeted for diagnostic and therapeutic purposes [27]. A prominent method used today to engage the tibialis anterior is FES-assisted gait training to prevent foot drop in the swing phase [4, 20, 33, 45]. The foot drop stimulation using implantable or surface electrodes are as equivalent as or even more effective than the ankle foot orthosis. However, implantation of intraneural electrodes requires experienced surgical skills and these surface electrode stimulation may increase prevalence of skin irritation [12, 24]. Anatomical researches focused on the motor end plate zones, NEPs, PMTJ, and DMTJ, must be the guidance to minimize surgical complications and skin problems when applying FES-assisted ankle dorsiflexion.

The electrodes for gait-assisting FES devices should be placed in relation to the NEPs, which were found to be located at 85–95 % of the distance from the lateral malleolus to the fibular head. The mean width of the muscle at its widest point, assumed to be at 70 % of the distance from the lateral malleolus to the fibular head, was 2.7 cm. The locations of the NEPs and the mean muscle width can be generalized to the larger population, as no significant differences among the specimens were found based on gender or nationality.

A prior cadaveric study that dissected 20 sides reported that the tibialis anterior is innervated by two to four NEPs

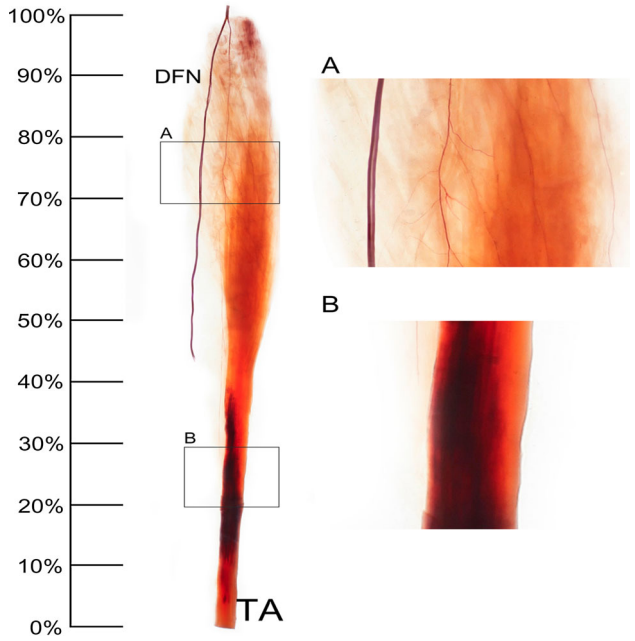

Fig. 3 The nerve distribution inside the tibialis anterior muscle is revealed by Sihler's staining. The arborized portion of the tibialis anterior was located at 70–80 % of the distance from the lateral malleolus. The most distal part of the nerve ending was at 25–30 % of the distance from the lateral malleolus, which was same distance as the distal musculotendinous junction. After the muscle was depigmented, the actual proximal musculotendinous junction was revealed at a mean distance of 78.2 % (instead of the topographic observation of 30.9 %) of the distance from the lateral malleolus. **a** The arborized portion of the nerve ending. **b** The most distal part of the nerve ending. *TA* tibialis anterior, *DFN* deep fibular nerve

branching out from the deep fibular nerve [36]. This report did not, however, state exactly the locations of the NEPs using anatomical indexes or proportions. Here, findings from 110 sides showed the presence of one to four NEPs per specimen with precise proportional locations based on index points.

Previous research using gait-assisted FES described the location of stimulation only vaguely. Adjustments in the placements of electrodes were recommended to stimulate the tibialis anterior more selectively to achieve the desired motion in both the sagittal and frontal planes [34, 42]. No detailed information about the locations of stimulation was given. Misplaced electrodes spaced too far apart promote deeper penetration of the current, causing plantar flexion by striking the tibialis posterior [2, 15, 34]. Likewise, the large size of the electrode can cause unintended stimulation of the fibularis muscles and evoke unintended plantarflexion and hypereversion of the ankle, which should be avoided in patients who have suffered a stroke [16, 22]. Springer et al. reported that isolated muscle activation of the tibialis anterior is necessary in cases of ankle hypereversion [44]. Ankle hypereversion may occur when electrodes are placed laterally, as NEPs of the tibialis anterior and fibularis longus (90 %) and brevis (72 %) overlap in the vertical range [25]. If stimulation of the common fibular nerve produces too much eversion of the ankle, the electrode can be relocated medially to stimulate the motor points of the tibialis anterior muscle [40].

The results reported here suggest that isolated contraction of the tibialis anterior should be performed selectively, with the electrodes located over the NEPs at 85–95 % of the distance from the lateral malleolus to the fibular head. Smaller electrodes should be used, as the tibialis anterior has a maximum muscle width of 2.73 cm.

By basing the general electrode placement for FES on the results of this anatomical study, clinicians can obtain low skin electrode impedance, which can lower the incidence of burning; conduct current uniformly; allow desired movement; and avoid skin irritation, thereby reducing pain and increasing effectiveness.

Varus deformity of the foot and ankle are common in patients with cerebral palsy, particularly those with hemiplegic-type neurologic impairments [37]. The tibialis posterior has been considered to be a main contributor to varus deformity in these patients [9]. Therefore, this muscle is frequently targeted for botulinum toxin injection in children with spastic cerebral palsy to reduce abnormal hypertonicity and to correct equinovarus deformity [38]. However, a higher prevalence of tibialis anterior spasticity and dysfunction as a contributor to varus foot deformity was reported in patients with cerebral palsy using dynamic electromyography [32]. Although the therapeutic effect of botulinum toxin injection to the tibialis anterior muscle for spastic varus deformity of the foot has not been studied sufficiently, the ideal sites of botulinum toxin injection to this muscle should be elucidated before performing clinical research.

While botulinum toxin has been used in various clinical fields for over 25 years, this treatment remains a challenge due to the complex considerations required before its application and its side effects [14]. Usually, side effects result from inaccurate injection and excessive diffusion. As the therapeutic effects of botulinum toxin are dependent on dosage, a sufficient amount of botulinum toxin should be delivered to the motor end plate zone of targeted muscle [50]. However, an overdose of botulinum toxin can cause it to spread to adjacent muscle and induce undesirable paralysis [18, 23, 26]. To lessen unwanted side effects and maximize the efficacy, botulinum toxin should be injected as close as possible to the motor end plate zones. Accordingly, a comprehensive knowledge of the locations of the motor end plate zones of the targeted muscle is a prerequisite for injecting toxin in a swift and accurate manner, and there has been much research performed on the anatomical locations of motor end plate zones for targeted muscles [7, 19, 26, 39, 43, 53].

The findings of the present study with regard to the intramuscular arborizing patterns of the deep fibular nerve in the tibialis anterior suggest optimum sites for botulinum toxin injection at 70–80 % from the lateral malleolus, where the arborized pattern was observed by Sihler's staining (Fig. 3a). Additionally, we could observe by depigmenting the muscle that the tendinous portion terminated at a mean of 78.2 % and became thicker distally, although the PMTJ was identified by dissection at a mean of 30.9 % from the lateral malleolus. The intramuscular tendon injury should be considered in clinical applications for the patients with muscle strains and the extents of post-injury musculotendon remodeling were correlated with likelihood of re-injury [8, 17]. Therefore, clinicians should avoid needling below about 70 % from the lateral malleolus so as not to penetrate the intramuscular tendon. However, ultrasonography with electrical stimulation guidance is helpful for more accurate and efficient injection.

Acknowledgments Kim and Rha contributed equally to this work as co-corresponding authors. This study was supported by a faculty research grant of Yonsei University College of Medicine in 2014 (6-2014-0140). The authors thank Sang-Hoon Kwon, Yong-Woong Lee, and Kevin Lee from the College of Arts and Science, New York University. We also thank In-Kyo Oh, who is majoring in Chemistry at the University of Western Ontario. These authors performed the English editing of manuscript.

Compliance with ethical standards

Conflict of interest I acknowledge that I have considered the conflict of interest statement included in "Author Guidelines". I hereby certify that, to the best of my knowledge, no aspect of my current personal or professional situation might reasonably be expected to significantly affect my views on the subject I am presenting. The authors declare that they have no conflict of interest.

Financial disclosure None of the authors have financial supports from commercial, academic, or political organizations or people regarding this study.

References

1. Bardeleben KHV, Haeckel E (1906) Atlas of applied (topographical) human anatomy for students and practitioners. Rebman limited, New York; Rebman Company, London
2. Benton LA, Rancho Los Amigos Rehabilitation Engineering C, National Institute of Handicapped R (1981) Functional electrical stimulation: a practical clinical guide. Rancho Los Amigos Rehabilitation Engineering Center, Rancho Los Amigos Hospital (7601 E. Imperial Hwy., Downey 90242), Downey, Calif
3. Bethoux F, Rogers HL, Nolan KJ, Abrams GM, Annaswamy TM, Brandstater M, Browne B, Burnfield JM, Feng W, Freed MJ, Geis C, Greenberg J, Gudesblatt M, Ikramuddin F, Jayaraman A, Kautz SA, Lutsep HL, Madhavan S, Meilahn J, Pease WS, Rao N, Seetharama S, Sethi P, Turk MA, Wallis RA, Kufta C (2014) The effects of peroneal nerve functional electrical stimulation versus ankle-foot orthosis in patients with chronic stroke: a randomized controlled trial. Neurorehabil Neural Repair 28:688–697
4. Bogataj U, Gros N, Kljajic M, Acimovic R, Malezic M (1995) The rehabilitation of gait in patients with hemiplegia: a comparison between conventional therapy and multichannel functional electrical stimulation therapy. Phys Ther 75:490–502
5. Burridge JH, Haugland M, Larsen B, Pickering RM, Svaneborg N, Iversen HK, Christensen PB, Haase J, Brennum J, Sinkjaer T (2007) Phase II trial to evaluate the ActiGait implanted drop-foot stimulator in established hemiplegia. J Rehabil Med 39:212–218
6. Chae J, Fang ZP, Walker M, Pourmehdi S (2001) Intramuscular electromyographically controlled neuromuscular electrical stimulation for upper limb recovery in chronic hemiplegia. Am J Phys Med Rehabil 80:935–941
7. Chantelot C, Feugas C, Guillem P, Chapnikoff D, Remy F, Fontaine C (1999) Innervation of the medial epicondylar muscles: an anatomic study in 50 cases. Surg Radiol Anat 21:165–168
8. Constantinou M, Wilson A (2004) Traumatic tear of tibialis anterior during a Gaelic football game: a case report. Br J Sports Med 38:e30
9. Coughlin MJ, Mann RA (1999) Surgery of the foot and ankle. Mosby, St. Louis
10. de Kroon JR, van der Lee JH, Ijzerman MJ, Lankhorst GJ (2002) Therapeutic electrical stimulation to improve motor control and functional abilities of the upper extremity after stroke: a systematic review. Clin Rehabil 16:350–360
11. Di Nardo F, Mengarelli A, Maranesi E, Burattini L, Fioretti S (2015) Assessment of the ankle muscle co-contraction during normal gait: a surface electromyography study. J Electromyogr Kinesiol 25:347–354
12. Dunning K, O'Dell MW, Kluding P, McBride K (2015) Peroneal stimulation for foot drop after stroke: a systematic review. Am J Phys Med Rehabil 94:649–664
13. Edwards P, Hsu J (1993) SPLATT combined with tendo achilles lengthening for spastic equinovarus in adults: results and predictors of surgical outcome. Foot Ankle 14:335–338
14. Evidente VG, Pappert EJ (2014) Botulinum toxin therapy for cervical dystonia: the science of dosing. Tremor Other Hyperkinet Mov (N Y) 4:273
15. Gersh MR (1992) Electrotherapy in rehabilitation. Davis, Philadelphia
16. Griffin JE, Karselis TC, Currier DP (1988) Physical agents for physical therapists. Thomas, Springfield, Ill., USA
17. Heiderscheit BC, Sherry MA, Silder A, Chumanov ES, Thelen DG (2010) Hamstring strain injuries: recommendations for diagnosis, rehabilitation, and injury prevention. J Orthop Sports Phys Ther 40:67–81
18. Hsu TS, Dover JS, Arndt KA (2004) Effect of volume and concentration on the diffusion of botulinum exotoxin A. Arch Dermatol 140:1351–1354
19. Hwang K, Jin S, Hwang SH, Lee KM, Han SH (2007) Location of nerve entry points of flexor digitorum profundus. Surg Radiol Anat 29:617–621
20. Hwang S, Jeon HS, Yi CH, Kwon OY, Cho SH, You SH (2010) Locomotor imagery training improves gait performance in people with chronic hemiparetic stroke: a controlled clinical trial. Clin Rehabil 24:514–522
21. Karabay I, Ozturk GT, Malas FU, Kara M, Tiftik T, Ersoz M, Ozcakar L (2014) Short-term effects of neuromuscular electrical stimulation on muscle architecture of the tibialis anterior and gastrocnemius in children with cerebral palsy: preliminary results of a prospective controlled study. Am J Phys Med Rehabil. doi:10.1097/PHM.0000000000000238
22. Kendall FP, Kendall FP (2005) Muscles: testing and function with posture and pain. Lippincott Williams & Wilkins, Baltimore

23. Kinnett D (2004) Botulinum toxin A injections in children: technique and dosing issues. Am J Phys Med Rehabil 83:S59–S64
24. Kottink AI, Tenniglo MJ, de Vries WH, Hermens HJ, Buurke JH (2012) Effects of an implantable two-channel peroneal nerve stimulator versus conventional walking device on spatiotemporal parameters and kinematics of hemiparetic gait. J Rehabil Med 44:51–57
25. Lee JH, Lee BN, An X, Chung RH, Kwon SO, Han SH (2011) Anatomic localization of motor entry point of superficial peroneal nerve to peroneus longus and brevis muscles. Clin Anat 24:232–236
26. Lepage D, Parratte B, Tatu L, Vuiller F, Monnier G (2005) Extra- and intramuscular nerve supply of the muscles of the anterior antebrachial compartment: applications for selective neurotomy and for botulinum toxin injection. Surg Radiol Anat 27:420–430
27. Levin O, Vanwanseele B, Thijsen JR, Helsen WF, Staes FF, Duysens J (2015) Proactive and reactive neuromuscular control in subjects with chronic ankle instability: evidence from a pilot study on landing. Gait Posture 41:106–111
28. Liberson WT, Holmquest HJ, Scot D, Dow M (1961) Functional electrotherapy: stimulation of the peroneal nerve synchronized with the swing phase of the gait of hemiplegic patients. Arch Phys Med Rehabil 42:101–105
29. Limpaphayom N, Chantarasongsuk B, Osateerakun P, Prasongchin P (2015) The split anterior tibialis tendon transfer procedure for spastic equinovarus foot in children with cerebral palsy: results and factors associated with a failed outcome. Int Orthop 39:1593–1598
30. Lyons GM, Sinkjaer T, Burridge JH, Wilcox DJ (2002) A review of portable FES-based neural orthoses for the correction of drop foot. IEEE Trans Neural Syst Rehabil Eng 10:260–279
31. Malouin F, Richards CL (2000) Preparatory adjustments during gait initiation in 4–6-year-old children. Gait Posture 11:239–253
32. Michlitsch MG, Rethlefsen SA, Kay RM (2006) The contributions of anterior and posterior tibialis dysfunction to varus foot deformity in patients with cerebral palsy. J Bone Joint Surg Am 88:1764–1768
33. Pease WS (1998) Therapeutic electrical stimulation for spasticity: quantitative gait analysis. Am J Phys Med Rehabil 77:351–355
34. Prosser LA, Curatalo LA, Alter KE, Damiano DL (2012) Acceptability and potential effectiveness of a foot drop stimulator in children and adolescents with cerebral palsy. Dev Med Child Neurol 54:1044–1049
35. Ramachandran M, Eastwood DM (2006) Botulinum toxin and its orthopaedic applications. J Bone Joint Surg Br 88:981–987
36. Reebye O (2004) Anatomical and clinical study of the common fibular nerve. Part 1: anatomical study. Surg Radiol Anat 26:365–370
37. Rha DW, Im SH, Lee SC, Kim SK (2010) Needle insertion into the tibialis posterior: ultrasonographic evaluation of an anterior approach. Arch Phys Med Rehabil 91:283–287
38. Rha DW, Park ES, Jung S, Lee SC, Suh M, Choi HS (2014) Comparison of ultrasound-guided anterior and posterior approaches for needle insertion into the tibialis posterior in hemiplegic children with spastic cerebral palsy. Am J Phys Med Rehabil 93:841–848
39. Roberts C, Crystal R, Eastwood DM (2006) Optimal injection points for the neuromuscular blockade of forearm flexor muscles: a cadaveric study. J Pediatr Orthop B 15:351–355
40. Robinson AJ, Snyder-Mackler L (2008) Clinical electrophysiology: electrotherapy and electrophysiologic testing. Wolters Kluwer Health/Lippincott Williams & Wilkins, Philadelphia
41. Sabut SK, Sikdar C, Kumar R, Mahadevappa M (2011) Improvement of gait and muscle strength with functional electrical stimulation in sub-acute and chronic stroke patients. Conf Proc IEEE Eng Med Biol Soc 2011:2085–2088
42. Sabut SK, Sikdar C, Mondal R, Kumar R, Mahadevappa M (2010) Restoration of gait and motor recovery by functional electrical stimulation therapy in persons with stroke. Disabil Rehabil 32:1594–1603
43. Sheverdin VA, Hur MS, Won SY, Song WC, Hu KS, Koh KS, Kim HJ (2009) Extra- and intramuscular nerves distributions of the triceps surae muscle as a basis for muscle resection and botulinum toxin injections. Surg Radiol Anat 31:615–621
44. Springer S, Braun-Benyamin O, Abraham-Shitreet C, Becher M, Laufer Y (2014) The effect of electrode placement and interphase interval on force production during stimulation of the dorsiflexor muscles. Artif Organs 38:E142–E146
45. Thrasher TA, Popovic MR (2008) Functional electrical stimulation of walking: function, exercise and rehabilitation. Ann Readapt Med Phys 51:452–460
46. Wilkenfeld AJ (2013) Review of electrical stimulation, botulinum toxin, and their combination for spastic drop foot. J Rehabil Res Dev 50:315–326
47. Won SY, Cho YH, Choi YJ, Favero V, Woo HS, Chang KY, Hu KS, Kim HJ (2015) Intramuscular innervation patterns of the brachialis muscle. Clin Anat 28:123–127
48. Won SY, Hur MS, Rha DW, Park HD, Hu KS, Fontaine C, Kim HJ (2010) Extra- and intramuscular nerve distribution patterns of the muscles of the ventral compartment of the forearm. Am J Phys Med Rehabil 89:644–652
49. Won SY, Kim SH, Kim ST, Paik DJ, Song WC, Koh KS, Chung MK, Kim HJ, Hu KS (2010) Trabecular bone ratio of mandible using micro-computed tomography in Korean. J Craniofac Surg 21:920–924
50. Won SY, Rha DW, Kim HS, Jung SH, Park ES, Hu KS, Kim HJ (2012) Intramuscular nerve distribution pattern of the adductor longus and gracilis muscles demonstrated with Sihler staining: guidance for botulinum toxin injection. Muscle Nerve 46:80–85
51. Yang HM, Won SY, Kim HJ, Hu KS (2013) Sihler staining study of anastomosis between the facial and trigeminal nerves in the ocular area and its clinical implications. Muscle Nerve 48:545–550
52. Yang HM, Won SY, Lee YI, Kim HJ, Hu KS (2014) The Sihler staining study of the infraorbital nerve and its clinical complication. J Craniofac Surg 25:2209–2213
53. Yi KH, Rha DW, Lee SC, Cong L, Lee HJ, Lee YW, Kim HJ, Hu KS (2015) Intramuscular nerve distribution pattern of ankle invertor muscles in human cadaver using Sihler stain. Muscle Nerve. doi:10.1002/mus.24939